Advanced Modulation Formats for Ultra-high-speed Transport Networks

Yikai Su and Lothar Möller*
State Key Lab of Advanced Optical Communication Systems and Networks, Shanghai Jiao Tong University, 800 DongChuan Rd, Shanghai, 200240, China, yikaisu@sjtu.edu.cn
*Bell Laboratories, Lucent Technologies, 791 Holmdel-Keyport Rd, NJ 07733, USA lmoeller@lucent.com

ABSTRACT

We discuss recent progress on ultra-high-speed modulation formats for next-generation optical transport networks at 160 Gb/s and beyond. In particular, we demonstrate CSRZ, PAP-CSRZ, GAP-CSRZ, RZ-VSB, and DPSK signals at ultra-high data rates.

Keywords: High speed, optical communications, modulation formats, nonlinear optics

1. INTRODUCTION

Since the invention and deployment of fiber-optic communication systems, the data rate of transmission systems has been historically increasing due to some inherent advantages of high-speed signaling. Typically, when the date rate quadruples the cost of electronic terminal equipments increases by a factor of 2.5. Thus a major benefit that high-speed systems bring in is the cost saving. With the same capacity in wavelength-division multiplexed (WDM) systems, ultra-high-speed systems offer reduced power consumption, minimized equipment footprint, and simplified network management due to the fewer number of wavelength channels.

Figure 1 is a plot showing the time when various generations of WDM transmission systems became commercially available[1]. The triangle data corresponds to the recent experimental result on the 85.4-Gb/s ETDM receiver reported in ECOC 2004[2], and the square data represents the most recent demonstration of 80-Gb/s ETDM transmitter in OFC 2005[3]. Clearly, the next data rate for product-relevant fiber-optic communications will be 160 Gb/s. Recently there have been a number of research results reported on 160-Gb/s systems based on optical time-division multiplexing (OTDM) approaches. In these experiments, phase-uncorrelated signals were employed due to the nature of the OTDM approach, where short pulses at lower rates are interleaved in time domain through the use of delay lines, which can cause drift in optical phases.

However, today all commercial ETDM systems run on phase correlated signals such as non return-to-zero (NRZ), return-to-zero (RZ), carrier suppressed RZ (CSRZ), duonary, and differentially phase shifted keying (DPSK). Phase-correlated signal formats can provide some significant advantages in linear and nonlinear transmission. In this paper we report recent progress on the generation of ultra-high-speed data signals for optical telecom applications. These formats include CSRZ, pairwise-alternating phase (PAP) CSRZ, group-alternating phase (GAP) CSRZ, RZ with vestigial sideband (VSB), and DPSK at 160 Gb/s rate and higher.

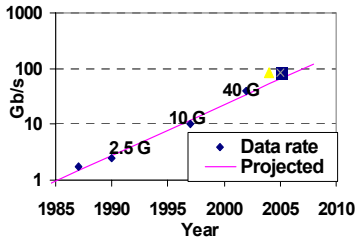

Fig. 1: Data rate increment of fiber-optic communications systems based on ETDM transceivers. Triangle: 85.4Gb/s ETDM receiver reported at ECOC 2004. Square: 80-Gb/s ETDM transmitter presented at OFC 2005.

Optical Transmission, Switching, and Subsystems III, edited by Rodney S. Tucker, Dominique Chiaroni, Wanyi Gu, Ken-ichi Kitayama, Proc. of SPIE Vol. 6021, 60210Q, (2005) · 0277-786X/05/$15 · doi: 10.1117/12.636024

2. ULTRA-HIGH-SPEED DATA-SIGNAL GENERATION

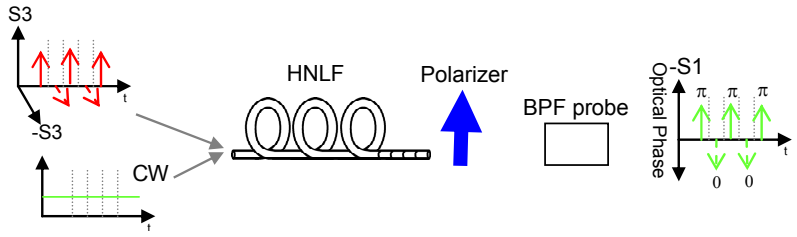

Fig.2: Principle of the Kerr shutter.

Recently an all-optical method was proposed to obtain phase-coherent ultra-high-speed signals by using an all-fiber based Kerr shutter[4,5]. This method is very effective in generating phase-correlated signals and performing phase modulation of ultra-short pulses. We first discuss the operation principle of the fiber Kerr shutter, which primarily consists of a piece of highly nonlinear fiber (HNLF) and a polarizer as shown in Fig.2. A high-speed optical data signal acts as the pump of the Kerr shutter, and a CW coherent signal is the probe. The pump data signal is aggregated from low rate data pulses by conventional OTDM means, and this non-coherent data signal interacts with the CW-light in the HLNF through the nonlinear polarization rotation (NLPR) process, which originates from cross phase modulation effects. At the output of the HNLF, a polarizer blocks the CW-light in absence of the pump signal. The polarization state of the probe wave is rotated if the pump is turned on. Therefore, a data pattern is carved out of the original CW-light. The new data pulses are phase-correlated since they are from a highly-coherent DFB laser. In addition, by controlling the polarization of the pump signals, phase modulation of the probe can be realized. For example, if the polarization of a pump pulse is rotated by 90º, the phase on the CW -light changes by π. By using this fiber-based Kerr shutter while controlling the pump polarization, we have generated various phase-correlated signal formats. The optical Kerr shutter is all-fiber based and capable of performing ultra-fast signal processing, the fundamental speed is limited to a few femtosecond, thus enabling ultra-high speed signaling extending to Tb/s range.

We have used this method to generate different signal formats such as 160-Gb/s conventional CSRZ with alternating phase between adjacent bits, and 160Gb/s PAP CSRZ with pair-wise alternating phases[6,7]. The two signals have similar pulse intensity profiles but the optical phase encoding schemes are different. For CSRZ, the signal is 0 π 0 π phase modulated with the pump pulses controlled in such a way that every other pump pulse is orthogonal polarized. While for PAP-CSRZ[8] the pump pulses are pair-wise orthogonal polarized resulting in a probe signal that is 0 0 π π phase modulated. We perform investigations on the nonlinear tolerance of CSRZ and PAP-CSRZ formats at 160 Gb/s through analytical studies, numerical simulation, and experimental verifications. The PAP-CSRZ outperforms the CSRZ by showing certain

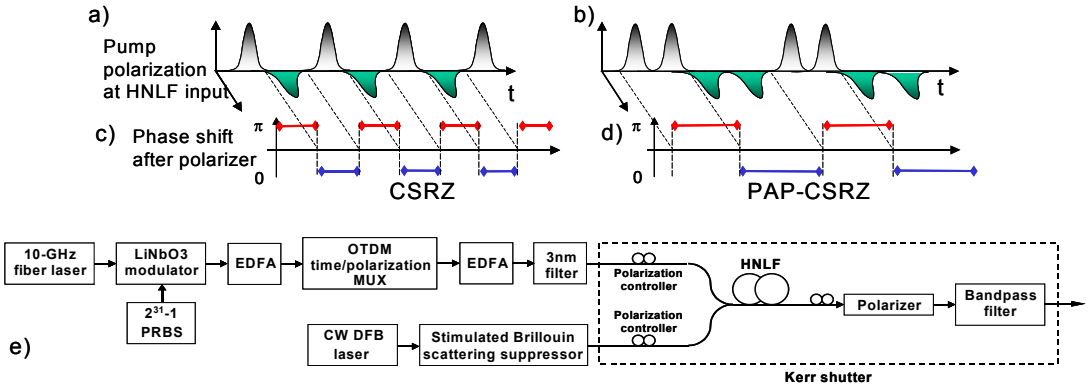

Fig. 3: Illustration of phase coding through polarization control of the pump pulses. a) alternating-polarization of non-coherent pump pulses, b) the resulting periodic phase shifts for CSRZ, c) pair-wise alternating polarization state, d) PAP-CSRZ, e) setup of the all-fiber based Kerr shutter.

improvement of nonlinear tolerance. Generation of 320-Gb/s CSRZ signal is also demonstrated; we believe this is the highest rate of CSRZ reported to date.

We first generate CSRZ and PAP-CSRZ signal at 160 Gb/s. The two schemes are depicted in Fig. 3 showing the pump polarizations and the corresponding phase shifts of the probe signals. When every other pump pulse is orthogonally polarized, the probe signal becomes 0 π 0 π phase-modulated resulting in a CSRZ format. If the pump pulses are pair-wise orthogonally polarized the probe signal is 0 0 π π phase modulated resulting in a PAP-CSRZ signal, as seen in Fig.3a-d. The line spacings for the two signals are 160 GHz and 80 GHz, respectively.

Fig.3e shows the schematic of the experimental setup. The 10-GHz actively mode-locked fiber laser outputs 2.2-ps pulses, which are externally modulated by a $LiNbO_3$ intensity modulator with a pseudo-random bit sequence (PRBS) of $2^{31} - 1$ length. A 160-Gb/s signal is formed by multiplexing the 10-Gb/s pulses. At the last stage of the OTDM multiplexer the polarization of the pump pulses are controlled in the way as sketched in Fig.3a-d for obtaining the desired signal formats. The HNLF has a length of 2.0 km, a Kerr nonlinearity coefficient of 12/W/km, and a zero dispersion of 1551 nm. The wavelengths of the pump and the CW probe are chosen to be 1546 nm and 1556 nm, respectively thus the group velocity of the pump and the probe signals are the same in the fiber. At the HNLF output a polarizer blocks the probe signal in absence of the pump. A band-pass filter selects only the probe wavelength for the subsequent detection by an OTDM receiver.

For generating the 160 Gb/s signals, the 10-Gb/s pulse train is multiplexed by three OTDM stages and then launched to the final polarization multiplexer stage. In the case of the 320-Gb/s CSRZ signal a fourth OTDM stage was added before the polarization multiplexing. Pump and signal powers at the input of the HLNF were 16-19dBm and 15-16dBm, respectively. The signal spectra are shown in Fig. 4 a-c, respectively. The autocorrelation trace of the CSRZ (Fig. 4d) signal shows a pulse width of ~1.4ps, which is also identical to that of the PAP-CSRZ. The 320-Gb/s CSRZ signal was generated by carefully compensating the chromatic dispersion of the OTDM unit and the EDFAs employed in the system resulting in an even smaller pulse width of 1.2 ps (Fig. 4e). The receiver provides a switching window of 3.5 ps for de-multiplexing 160-Gb/s data signals and is based on a typical OTDM scheme, mainly consisting of several EDFAs for pre-amplification and loss compensation, bandpass filters for ASE suppression, and an 40GHz electro-absorption modulator (EAM) followed by an 40-Gb/s electrical receiver. The BER was measured at 10 Gb/s. Monitoring the probe signal spectrum behind the polarizer with an OSA helps to adjust the SOP and power of the launched pump signal at the input of the HNLF (symmetrical shape, maximum power). In the experiment the sensitivities of the tributaries were checked and they have shown similary performance.

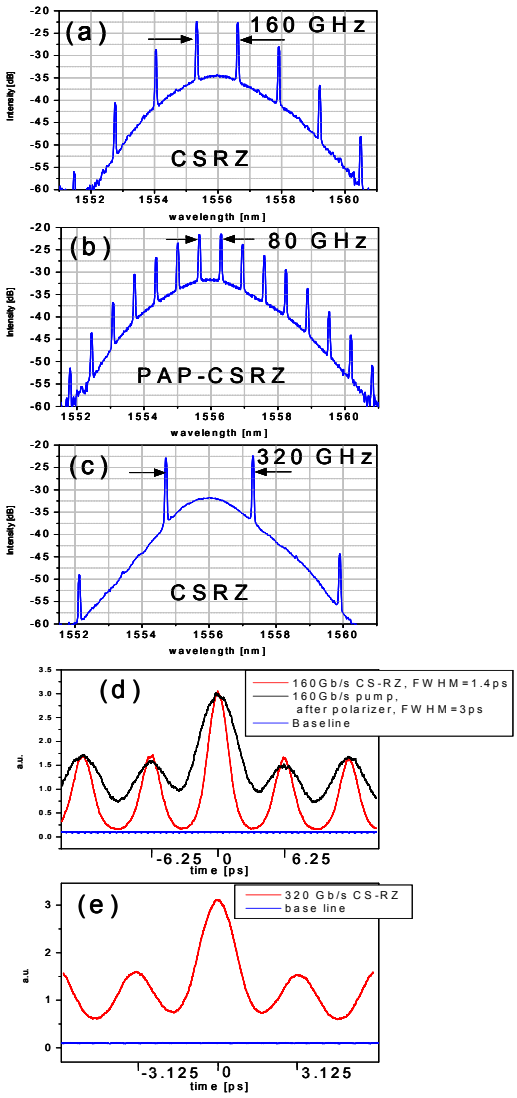

Fig. 4: Spectra of a) the 160-Gb/s CSRZ signal, b) the 160-Gb/s PAP-CSRZ signal, and c) the 320-Gb/s CSRZ signal, d) shows the autocorrelation traces of the 160-Gb/s signals, and e) is the autocorrelation of the 320-Gb/s CSRZ signal.

To compare the nonlinear performance of the PAP-CSRZ and CSRZ formats, we used a 38-km single-mode fiber (SMF) transmission span with 100% post dispersion compensation. Fig.5 shows the receiver sensitivity penalties versus the signal launch powers in the SMF for both formats. Compared to the conventional CSRZ signal, the PAP-CSRZ signal

exhibits improvement in tolerance to intra-channel nonlinear impairments. The improvement could also be explained by

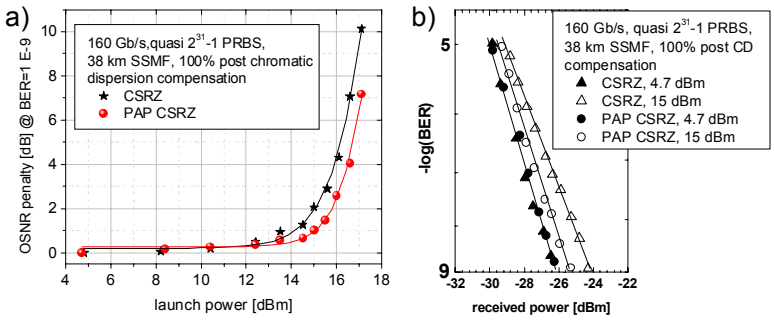

Fig. 5: a) sensitivity penalty due to NL propagation, b) BER curves.

simulations[8] and analytical studies[9].

We also describe some recently demonstrated applications of 160-Gb/s formats that were generated by means of the aforementioned the Kerr shutter. By strong filtering of phase-correlated RZ signal format with VSB, 0.8-bit/s/Hz spectral efficiency can be achieved at such high rate. The required phase-correlated RZ signal is obtained by simply controlling the pump pulses to be collinearly polarized, and a micro-electromechanical system (MEMS) based blocker filter, whose bandwidth and center wavelength can be set in steps of 13 GHz, is used to find the optimal filter conditions for the signal.

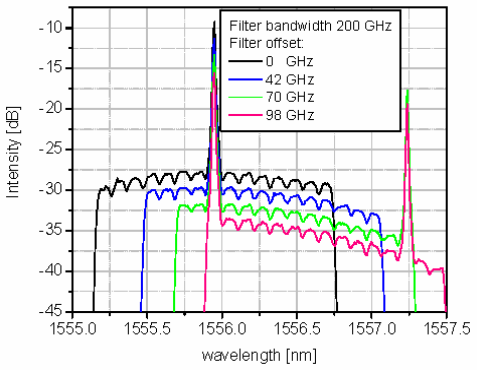

Fig. 6: RZ-VSB signals with different filter offsets.

The filter has a rectangular passband, and a good suppressing ratio of >30 dB. In addition, the square-like filter shape minimizes the required guard bands between WDM channels. The filter bandwidth is set to ~200 GHz so the spectral efficiency for the 160-Gb/s signal is 0.8 bit/s/Hz. Fig. 6 shows the spectra of the filtered signals with different filter offsets. Best performance was observed when the filter offset is approximately 70 GHz[10], where error-free operation was achieved.

Figure 7a shows the modulation scheme of the GAP-CSRZ format[11]. The phase modulation is performed in groups of every four bits. In Fig. 7b the optical spectrum of the corresponding simulated GAP-CSRZ signal is plotted. Note that the line spacing in the spectrum is 40 GHz, allowing us to spectrally filter the two closely spaced tones to recover the clock. The experimental setup is similar to that described in the PAP-CSRZ signal generation experiments. The auto-correlation trace indicates a pulse width of 1.8 ps with the converted GAP-CSRZ pulses. As shown in Fig. 8, the signal passes through a narrowband filter that selects two tones spaced by 40 GHz, and the corresponding electrical signal after the photo detection is provided in Fig. 8c showing a repetition rate of 40 GHz. A high-Q electric filter with a Q-value of ~1000 further selects the 40-GHz clock tone. The recovered clock waveform is shown in Fig. 8d. The clock processes a measured timing jitter of 330 fs including a 190-fs inherent jitter of the oscilloscope (Agilent 86107A) operated in the precision timing mode. Compared with the ~300-fs jitter of the MLL in the transmitter, the very small amount of the additional jitter would not cause receiver sensitivity penalty based on our previous measurements.

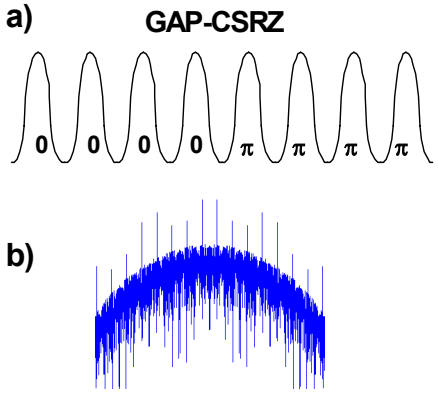

Fig. 7: Phase modulation of a) GAP-CSRZ and b) the resulting spectrum when data modulation is applied.

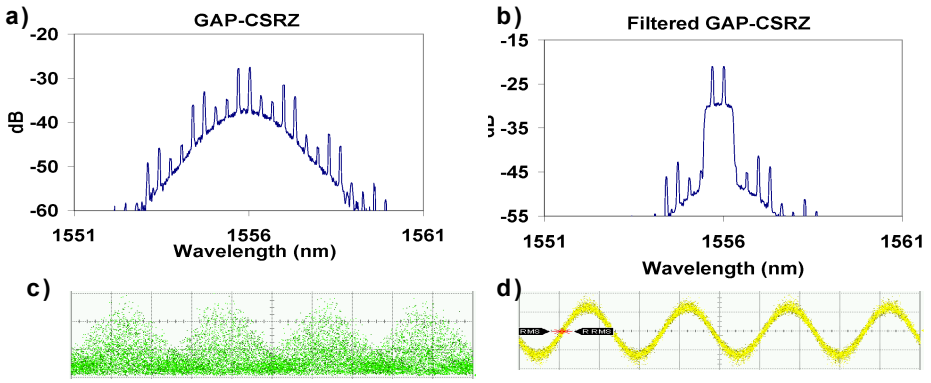

Fig.8: a) GAP-CSRZ spectrum, b) the filtered spectrum, c) the eye diagram of the filtered signal, and d) the recovered clock.

We now discuss the generation of fully phase correlated a DPSK format[12], which requires an additional signal

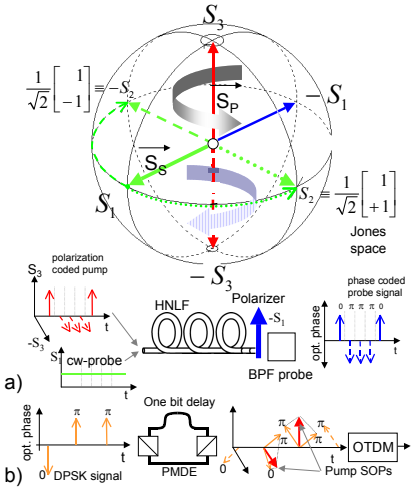

Fig.9: a) Polarization evolution through NLPR on the Poincaré sphere and b) polarization modulation based on DPSK.

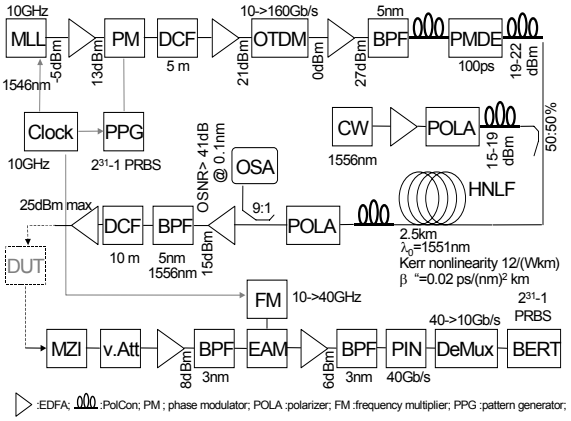

Fig.10: Experimental setup and its operation parameters.

processing step. The operation principle of our setup can be conveniently explained by means of polarization state evolutions on the Poincare sphere (fig.9a). NL polarization rotation (NLPR) between a strong pump and a weak probe signal forces the probe's state of polarization (SOP) $\mathbf{S_S}$ to move along the Poincare sphere's equator, when the launch SOP vectors of probe and pump ($\mathbf{S_P}$) equal $+\mathbf{S_1}$ and $+\mathbf{S_3}$, respectively. The probe's SOP rotates clockwise (counter clockwise) when the pump SOP points to $-\mathbf{S_3}$ ($+\mathbf{S_3}$) and its derivation angle depends on the pump power, fiber non-linearity and propagation length. For the sake of simplicity we assume a probe SOP pointing to either $+\mathbf{S_2}$ or $-\mathbf{S_2}$ when the NLPR process stops at the fiber end. These two SOPs correspond in Jones space to the field vectors $\mathbf{E_+}=\{E_x, E_y\}=[1,1]$ and $\mathbf{E_-}=[1,-1]$. Hence by selecting the vector's Ey component using a polarizer a 0-π phase-modulated signal originates when the pump SOP is switched between $+/-\mathbf{S_3}$. Finally, a bandpass filter after the polarizer separates the probe from the pump signal. The SOP-modulated pump signal is generated by launching a DPSK modulated pulse train at a low bit rate through a PMD emulator (PMDE) with a DGD equivalent to the pulse repetition rate (fig.9b). At its output the two DPSK signal replicas, delayed in time with respect to each other, build up two orthogonal SOPs, whose orientations are determined by the phase difference between the two superimposed pulses. A following OTDM unit up-converts the signal's data rate. The advantage of the approach is that starting from a low speed DPSK signal an ultra-high speed but incoherent SOP modulated pump signal is formed. This pump light can carve a 160-Gb/s DPSK signal from a coherent CW probe via the NLPR process without the need of ultra-high speed electronics.

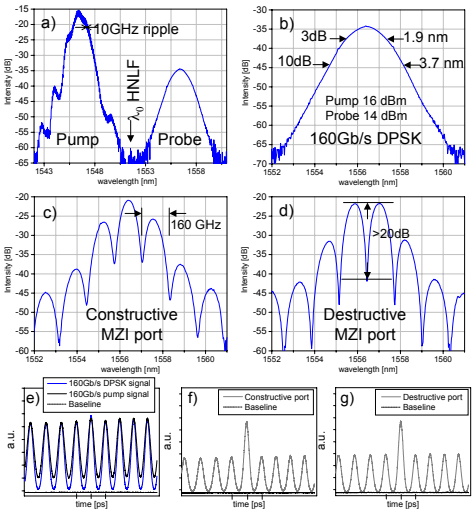

Fig.11: a-d) measured spectra as described in text, and e-g) auto-correlation traces (peak spacing corresponds to 6.25 ps).

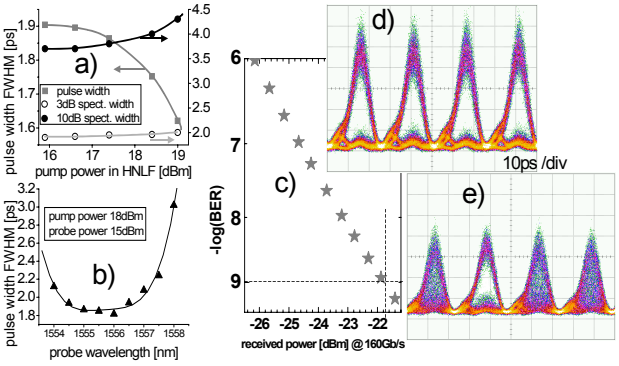

Fig.12: a) power dependent probe pulse widths; b) pulse width adjustment by tuning the probe wavelength; c) typical receiver sensitivity; d) 40Gb/s de-muxed DPSK eyes; e) 40Gb/s de-muxed OTDM interleaved DPSK eyes.

A detailed schematic including main operation parameters of the setup is shown in Fig.10. A hybrid electrically mode locked laser (MLL, 10 GHz repetition rate) produces pulses with 1.7-ps FWHM that are externally 0 or π phase modulated with a 2^{31}-1 PRBS at a 10-Gb/s data rate using a Mach-Zehnder modulator. OTDM modules convert the signal to a 160-Gb/s quasi PRBS. This single-polarized signal is superimposed with a delayed replica of itself that has equal power but orthogonal polarization in a PMDE with exactly 100-ps DGD. Thus, an SOP-modulated signal with 160-Gb/s data rate is obtained. The pump signal (1546 nm) is launched together with a CW wave (1556 nm) in a 2.5-km long HNLF (low PMD, zero dispersion wavelength at 1551 nm). Pump and probe signals are separated after the polarizer with a 5-nm wide bandpass filter. Decoding and detection of the 160-Gb/s RZ-DPSK signal were done by using an MZI with a delay of 6.25 ps, equivalent to a one bit delay, in one arm. Its single-ended output was launched into an optically pre-amplified OTDM receiver which design ahs been described before.

Fig. 11 shows spectra of the pump (*a*) and 160-Gb/s DPSK signal (*b*) after the polarizer. Ripples on top of the pump spectrum are caused by the filter effect that is generated by the PMDE and polarizer. Typically, the 3-dB and 10-dB bandwidths of the DPSK signal are around 1.9 nm and 3.7 nm, respectively at 16-dBm pump power. While the 3-dB bandwidth is almost pump power independent the 10-dB width slightly increases with higher pump power. Spectra (fig.11c/d) of the constructive and destructive MZI ports show its 160-GHz free spectral range (FSR), corresponding to one bit delay, and a contrast ratio >20 dB.

Auto correlation traces (fig.11e) reveal pulse widths of 2.4 ps for the pump at the HLNF input and 1.8 ps to 1.6 ps for the probe signal at the HNLF output at pump power levels between 16 and 19 dBm, respectively (Fig. 12a). Its shorter duty cycle compared to the pump can be explained by the power dependent NLPR process. Both traces at the MZI output ports (fig.11 f/g) look similar and indicate a high extinction ratio for the ON/OFF modulated signal that has the same pulse width as the DPSK signal before demodulation. The DPSK signal's pulse width varies (Fig.12b, equivalent to a duty cycle shift from 27 to 50%) by changing the wavelength offset of the probe relative to the HNLF's λ_0 because this causes a group velocity mismatch between pump and probe pulses.

BER measurements were performed by noise loading the optically pre-amplified receiver. Error-free operation (BER = $1x10^{-9}$) could be achieved with a typical launch power of around –22 dBm for the 160-Gb/s signal (Fig. 12c). Tributaries at the constructive and destructive ports performed similarly. We measured 340-fs rms timing jitter for the MLL output signal [13] and around 500-fs for the de-multiplexed 40 Gb/s on the receiver side. The low jitter MLL is one of the main improvements compared to our previous setup, which was timing jitter limited at low BER. The eye diagram (fig.12d) after optical de-multiplexing was recorded at the receiver sensitivity level and clearly shows that all four eyes look open and similar. Due to temperature shielding of the HNLF the source stays stable over several minutes.

In contrast to this we show the eyes of the single polarized pump signal after MZI de-modulation in order to make the qualitative difference between our fully phase-correlated format and a time-interleaved DPSK format visible. This OTDM 16x10Gb/s DPSK signal is equivalent to the formats reported before by other groups regarding its structure. However, after de-modulation using our one-bit MZI only one open eye became visible even when the MZI and OTDM units were fine-tuned (fig.12e). Note our signal can be also de-modulated with other MZI, i.e. that possess FSRs of 80, 40, or 10 GHz.

Conclusion

We review recent results[14] on 160-Gb/s phase-correlated signals including CSRZ, PAP-CSRZ, GAP-CSRZ, RZ-VSB, and DPSK for applications in future transport networks. The generation of these formats is based on an all-optical Kerr shutter. The details of investigating these formats and their performance are discussed.

REFERENCES

1. Govind P. Agrawal, "Fiber-optic communication systems," *Wiley-Interscience*, 1997
2. K. Schuh, B. Junginger, E. Lach, A. Klekamp, and E. Schlag, "85.4 Gbit/s ETDM receiver with full rate electronic clock recovery circuit," in *Proc. ECOC* 2004, post-deadline paper Th4.1.1.
3. Yichuan Yu et al., "80Gb/s ETDM transmitter with a traveling-wave electroabsorption modulator," in *Proc. OFC* 2005, paper OWE1.
4. Govind P. Agrawal, "Nonlinear fiber optics," *Academic Press*, 1995
5. Lothar Möller, Yikai Su, Xiang Liu, Juerg Leuthold, Chongjin Xie, "Ultra high-speed Optical Phase Correlated Data Signals,"*IEEE Photonics Technology Letters,* vol. 15, no. 11, pp 1597-1599, 2003
6. Lothar Möller, Yikai Su, Chongjin Xie, Roland Ryf, Xiang Liu, Xing Wei, and Steven Cabot, "All-optical phase construction of ps-pulses from fiber lasers for coherent signaling at ultra-high data rates (≥160 Gb/s)" in *Proc. OFC* 2004, paper PDP20, 2004.
7. Yikai Su, Lothar Möller, Chongjin Xie, Roland Ryf, Xiang Liu, Xing Wei, and Steven Cabot, "Ultra-high Speed Data Signals with Alternating and Pair-Wise Alternating Optical Phases," *IEEE/OSA J. Lightwave Technol.* Invited paper, vol. 23, no.1 2005, pp 26-31
8. S. Randel, B. Konrad, A. Hodzic, K. Petermann, "Influence of bitwise phase changes on the performance of 160 Gbit/s transmission systems," in *Proc. ECOC* 2002, paper P3.31, 2002.
9. X. Wei and X. Liu, "Analysis of intrachannel four-wave mixing in differential phase-shift keying transmission with large dispersion," *Opt. Lett*., vol. 28, no. 23, pp. 2300-2302, 2003

10. Yikai Su, Lothar Möller, Roland Ryf, Xiang Liu, and Chongjin Xie, "Feasibility study of 0.8bit/s/Hz spectral-efficiency at 160 Gb/s using phase-correlated RZ signal with vestigial sideband filtering," *IEEE Photonics Technology Letters*, vol. 16, no. 5, pp 1388-1390, May 2004
11. Yikai Su, Lothar Möller et al., "Demonstration of a 160-Gb/s group-alternating phase CSRZ format featuring simplified clock recovery and improved nonlinear performance," in *Proc. OFC* 2005, paper OFG3.
12. Lothar Möller, Yikai Su, Chongjin Xie, Roland Ryf et al., "Generation of a 160-Gb/s RZ-DPSK Signal and Its Detection with a One-Bit Mach-Zehnder Interferometer," in *Proc. ECOC* 2004, postdeadline paper Th4.4.6.
13. L. Möller, Y. Su, C. Xie, X. Liu, J. Leuthold, D. Gill, X. Wei, "Generation and detection of 80 Gb/s RZ-DPSK signals," Opt. Lett., 2003, pp. 2461-3.
14. Lothar Möller et al., "Enabling 160 Gbit/s transmitter and receiver designs," in *Proc. OFC* 2005 invited paper.